Maximum Ergodic Capacity of Intelligent Reflecting Surface Assisted MIMO Wireless Communication System

Chang Guo[1,3], Zhufei Lu[2], Zhe Guo[3], Feng Yang[1(✉)], and Lianghui Ding[1]

[1] Department of Electronic Engineering, Shanghai Jiao Tong University, Shanghai, China
{13122152125,yangfeng,lhding}@sjtu.edu.cn
[2] Yichang Testing Institute of Technology Research, Hubei, China
flypeter@126.com
[3] CETC Key Laboratory of Data Link Technology and Shanghai Microwave Research Institute, Shanghai, China
guozhe@foxmail.com

Abstract. Intelligent reflecting surface (IRS) is currently adopted by massive multiple-input multiple-output (MIMO) systems as a new expansion scheme. It effectively copes with the increasing cost and energy consumption. In this paper, we concentrate on an IRS-assisted MIMO system, in which the base station, IRS and user are all equipped with multiple antennas. We first give the upper bound of the ergodic capacity of the system. Then we maximize this upper bound and obtain the sub-optimal phase shifts of IRS by applying semi-definite relax and Gaussian random methods. Numerical results shows the advantage of the proposed solution and the performance increase brought by multiple antennas.

Keywords: Intelligent reflecting surface · Massive multiple-input multiple-output · Ergodic capacity · Semi-definite relax

1 Introduction

Massive multiple-input multiple-output (MIMO) is an essential and widely used technology in the fifth-generation (5G) communication system [12]. As the number of antennas increases, more spatial degrees of freedom can be used to greatly improve the performance of the communication system [13]. However, the increasing number of antennas also has an impact on the energy consumption, the overall system complexity as well as the hardware cost [1,13]. Therefore, energy efficiency and hardware cost need to be addressed in future constructions of wireless networks [15].

This paper is supported in part by NSFC China (61771309, 61671301, 61420106008, 61521062), Shanghai Key Laboratory Funding (STCSM18DZ1200102) and CETC Key Laboratory of Data Link Technology Foundation (CLDL-20162306).

H. Gao et al. (Eds.): ChinaCom 2019, LNICST 312, pp. 331–343, 2020.
https://doi.org/10.1007/978-3-030-41114-5_25

Intelligent reflecting surface (IRS), also known as large intelligent surface (LIS), has been introduced to massive MIMO systems as a new expansion scheme [7]. Specifically, IRS can be treated as a reflection plane composed of a set of passive components, such as varactor diodes [11] and devices with special materials [2,8]. Owing to the different electromagnetic and material properties of the components, the elements of IRS can be controlled by signals to generate different electromagnetic responses, making it possible to adjust the phase shifts of the reflected signals.

The IRS-assisted system has large advantages of cost and energy consumption. In addition, IRS is convenient to introduce to the current massive MIMO systems because it can be easily placed on or removed from various surfaces [14]. By adjusting the phase shifts of the IRS, the signals reflected by IRS can be an effective link supplement for the system, thus achieving signal power enhancement or interference signals suppression.

Currently, researches have been conducted on the deployment of IRS in actual scenarios and joint beamforming design. The work led by Xin showed that the use of IRS can achieve higher spectral space efficiency without any addition payload of the hardware and software at the user by developing an experimental test platform [17]. The research led by Wu studied an IRS-enhanced point-to-point multiple-input single-output (MISO) wireless system by jointly optimizing active transmit beamforming at the base station (BS) and passive reflected beamforming at the IRS [16]. Han obtained a closed form solution of the optimal phase shifts of a MISO system by introducing a strict approximation of ergodic capacity of IRS-assisted large-scale antenna systems [6]. In the work of Huang, the transmission power and IRS reflection phase shifts are designed with the aim of maximizing the achievable rate. Under the same energy consumption, the system throughput increases a lot compared to the system without IRS [10].

Previous researches also focuses on other aspects such as energy efficiency and physical layer security. Huang's work maximized energy and spectral efficiency, which has large advantages comparing to traditional amplified and forward (AF) relay [9]. The IRS-assisted system also contributes to physical layer security of wireless communication systems [3,18], which maximized the safe reception rate. The introduction of IRS brought more degrees of freedom to solve the problem of secure transmission in special scenarios.

Existing works mainly focus on the beamforming problem of the IRS-assisted system with multi-antenna at the BS and IRS, without considering multi-antenna at the user. In reality, the application of multiple antennas at the user helps increase the system capacity significantly. In this paper, we consider an IRS-assisted communication system that the BS, IRS and user all have multiple antennas. We analyze the upper bound of the ergodic capacity and formulate a problem of maximizing this upper bound. Considering the problem is not convex and hard to solve, we transform it into a convex semi-definite programming (SDP) problem by using semi-definite relax (SDR) method. The SDP problem can be easily solved by the optimization methods such as interior point method. Gaussian random method is used to decompose the optimal phase shifts of IRS

from the optimal solution. Through numerical simulation, we prove the advantages of the proposed solution and the result shows additional gains provided by multi-antenna system.

The rest of this paper is organized as follows, in Sect. 2, the system model is given, which consists of the channel model and the ergodic capacity. In Sect. 3, we analyze the upper bound of ergodic capacity and obtain the optimal solution by solving the problem of maximizing the the upper bound of ergodic capacity. In Sect. 4, we verify the analysis by numerical simulation. Finally, conclusion is drawn in Sect. 5.

Notations: Vectors and matrices are denoted by bold lowercase and uppercase letters, respectively. For a vector $\mathbf{v}$, $\mathrm{diag}(\mathbf{v})$ represents a diagonal matrix consists of corresponding element of $\mathbf{v}$. $\arg(\mathbf{v})$ represents the phase vector of $\mathbf{v}$. For a matrix $\mathbf{V}$, $\mathbf{V} \in \mathbb{C}^{m\times n}$ represents that the row and column of $\mathbf{V}$ are m and n. $\mathbf{V} \succeq 0$ represents $\mathbf{V}$ is a semi-definite matrix. $\mathbf{V}^H$, $\mathrm{rank}(\mathbf{V})$, $\mathrm{rvec}(\mathbf{V})$, $\mathbf{V}^i$ and $\mathbf{V}_{ij}$ denote the conjugate transpose, rank, row vectorization, the i-th column and the (i, j)-th element of a general matrix $\mathbf{V}$, respectively. $\det(\mathbf{S})$, $\mathrm{tr}(\mathbf{S})$ and $\mathbf{S}^{-1}$ denote the determinant, trace and inverse of a square matrix $\mathbf{S}$, respectively. $\mathbf{I}_K$ denotes K-order unit matrix, $\mathbb{E}\{\cdot\}$ denotes the statistical expectation, and $\mathcal{CN}(\mu, \sigma^2)$ denotes circular symmetric complex Gaussian distribution with mean μ and variance σ^2.

2 System Model

As shown in Fig. 1, we consider an IRS-assisted downlink MIMO wireless communication system, which consists of a base station (BS) equipped with M ($M = M_r \times M_c$) antennas and a user equipped with L ($L = L_r \times L_c$) antennas. There is an IRS assisting to transmit information between the BS and the user, which equipped by N ($N = N_r \times N_c$) reconfigurable reflection elements. Each element can apply different reflect phase shifts through a controller that connected to the BS.

We model the multiple antennas as a uniform rectangular array (URA). The wavelength of transmission signals is λ and the distance of adjacent antennas is d. Then the response of a URA with K ($K = K_r \times K_c$, K_r and K_c denote the row and column) elements can be denoted by $\mathbf{A}(x^{(h)}, x^{(v)}, K_r, K_c) \triangleq \left(e^{j\phi(x^{(h)}, x^{(v)}, m, n)}\right)_{m=1,\cdots,K_r, n=1,\cdots,K_c} \in \mathbb{C}^{K_r\times K_c}$, where $\phi(x^{(h)}, x^{(v)}, m, n)$ represents the phase difference between the (m, n)-th element and the (1, 1)-st element of the IRS, denoted by

$$\phi(x^{(h)}, x^{(v)}, m, n) \triangleq 2\pi\frac{d}{\lambda}\sin x^{(v)}\left((m-1)\cos x^{(h)} + (n-1)\sin x^{(h)}\right), \quad (1)$$

where $x^{(h)}$ and $x^{(v)}$ represent the horizontal and vertical angle of departure or arrival (AoD or AoA) of transmission signals, respectively. Denote the response of the URA as a vector, i.e, $\mathbf{a}\left(x^{(h)}, x^{(v)}, K_r, K_c\right) \triangleq \mathrm{rvec}\left(\mathbf{A}(x^{(h)}, x^{(v)}, K_r, K_c)\right) \in \mathbb{C}^{1\times K}$.

Generally, the IRS is installed on the wall of high buildings. Considering scattering is often rich, the channel from the BS to the IRS and the channel from the IRS to the user can be modeled in Rician fading, denoted by $\mathbf{H}_{bi} \in \mathbb{C}^{M\times N}$ and $\mathbf{H}_{iu} \in \mathbb{C}^{N\times L}$, i.e.,

$$\mathbf{H}_{bi} = \sqrt{\alpha_{bi}}\left(\sqrt{\frac{\mathcal{K}_{bi}}{\mathcal{K}_{bi}+1}}\bar{\mathbf{H}}_{bi} + \sqrt{\frac{1}{\mathcal{K}_{bi}+1}}\tilde{\mathbf{H}}_{bi}\right), \tag{2}$$

$$\mathbf{H}_{iu} = \sqrt{\alpha_{iu}}\left(\sqrt{\frac{\mathcal{K}_{iu}}{\mathcal{K}_{iu}+1}}\bar{\mathbf{H}}_{iu} + \sqrt{\frac{1}{\mathcal{K}_{iu}+1}}\tilde{\mathbf{H}}_{iu}\right), \tag{3}$$

where $\mathcal{K}_{bi}$, $\mathcal{K}_{iu}$ denote the Rice factors, α_{bi}, α_{iu} denote the distance-dependent path losses, $\tilde{\mathbf{H}}_{bi}$, $\tilde{\mathbf{H}}_{iu}$ denote the non-line-of-sight (NLoS) components and each element of them follows $\mathcal{CN}(0,1)$, $\bar{\mathbf{H}}_{bi}$, $\bar{\mathbf{H}}_{iu}$ denote the line-of-sight (LoS) components, which can be expressed as

$$\bar{\mathbf{H}}_{bi} = \mathbf{a}^H\left(\gamma_{bi}^{(h)}, \gamma_{bi}^{(v)}, M_r, M_c\right)\mathbf{a}\left(\delta_{bi}^{(h)}, \delta_{bi}^{(v)}, N_r, N_c\right), \tag{4}$$

$$\bar{\mathbf{H}}_{iu} = \mathbf{a}^H\left(\gamma_{iu}^{(h)}, \gamma_{iu}^{(v)}, N_r, N_c\right)\mathbf{a}\left(\delta_{iu}^{(h)}, \delta_{iu}^{(v)}, L_r, L_c\right), \tag{5}$$

where $\gamma_{bi}^{(h)}$, $\gamma_{bi}^{(v)}$ denote the horizontal AoD and vertical AoD from the BS, $\delta_{bi}^{(h)}$, $\delta_{bi}^{(v)}$ denote the horizontal AoA and vertical AoA to the IRS, $\gamma_{iu}^{(h)}$ and $\gamma_{iu}^{(v)}$ denote the horizontal AoD and vertical AoD from the IRS, $\delta_{iu}^{(h)}$ and $\delta_{iu}^{(v)}$ denote the horizontal AoA and vertical AoA to the user.

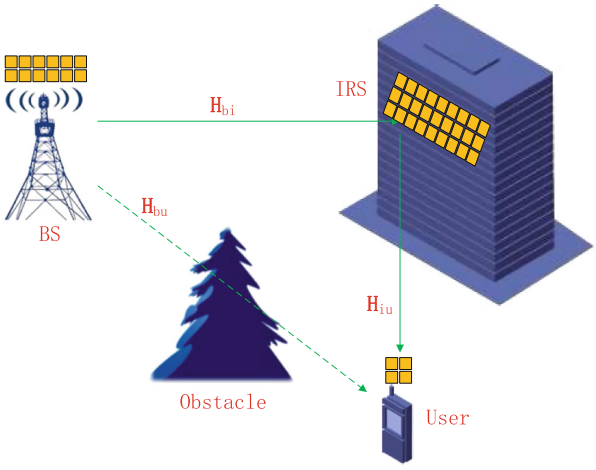

Fig. 1. System model

In addition, owing to the distance from the BS to the user is always far, the LoS may be blocked by obstacles. Thus, the channel between them is modeled in Rayleigh fading, denoted by $\mathbf{H}_{bu} \in \mathbb{C}^{M\times L}$, i.e.,

$$\mathbf{H}_{bu} = \sqrt{\alpha_{bu}}\tilde{\mathbf{H}}_{bi}, \tag{6}$$

where α_{bu} denotes the distance-dependent path loss, $\tilde{\mathbf{H}}_{bi}$ denotes the NLoS components and each element of $\tilde{\mathbf{H}}_{bi}$ follows $\mathcal{CN}(0,1)$.

Let $\boldsymbol{\Theta} = (\theta_{m,n})_{m=1,\cdots,N_r,n=1,\cdots,N_c} \in \mathbb{C}^{N_r \times N_c}$, where $\theta_{m,n}$ denotes the phase shift of the (m,n)-th element of the IRS. Define $\boldsymbol{\Phi} \triangleq \text{diag}(\text{rvec}(e^{j\boldsymbol{\Theta}})) \in \mathbb{C}^{N \times N}$. Thus, the equivalent channel, denoted by $\mathbf{H}(\boldsymbol{\Phi}) \in \mathbb{C}^{M \times L}$, can be expressed as

$$\mathbf{H}(\boldsymbol{\Phi}) = \mathbf{H}_{bi}\boldsymbol{\Phi}\mathbf{H}_{iu} + \mathbf{H}_{bu}. \tag{7}$$

For a given MIMO channel, the capacity is given by [4]. Therefore, the ergodic capacity of the IRS-assisted system can be expressed as

$$C(\boldsymbol{\Phi}) = \mathbb{E}\left\{\log_2 \det\left(\mathbf{I}_L + \rho\mathbf{H}^H(\boldsymbol{\Phi})\mathbf{H}(\boldsymbol{\Phi})\right)\right\}, \tag{8}$$

where $\rho = \frac{SNR}{M}$ and SNR denotes the average signal-to-noise ratio (SNR).

3 Ergodic Capacity Analysis and Optimization

In this section, we analyze the ergodic capacity of the system at first. Then we formulate an optimization problem based on the ergodic capacity and give the solution.

3.1 Ergodic Capacity Analysis

By applying Jensen Inequality, the upper bound of ergodic capacity of the IRS-assisted system is given by the following theorem.

Theorem 1.

$$\begin{aligned} C(\boldsymbol{\Phi}) \leqslant \log_2 \det(&\rho\beta_1 \bar{\mathbf{H}}_{iu}^H \boldsymbol{\Phi}^H \bar{\mathbf{H}}_{bi}^H \bar{\mathbf{H}}_{bi} \boldsymbol{\Phi} \bar{\mathbf{H}}_{iu} \\ &+ \rho\beta_2 M \bar{\mathbf{H}}_{iu}^H \bar{\mathbf{H}}_{iu} + (1 + \rho(\beta_3 MN + \beta_4 M))\mathbf{I}_L), \end{aligned} \tag{9}$$

where

$$\begin{aligned} \beta_1 &= \frac{\alpha_{bi}\alpha_{iu}\mathcal{K}_{bi}\mathcal{K}_{iu}}{(\mathcal{K}_{bi}+1)(\mathcal{K}_{iu}+1)}, \qquad \beta_3 = \frac{\alpha_{bi}\alpha_{iu}}{\mathcal{K}_{iu}+1}, \\ \beta_2 &= \frac{\alpha_{bi}\alpha_{iu}\mathcal{K}_{iu}}{(\mathcal{K}_{bi}+1)(\mathcal{K}_{iu}+1)}, \qquad \beta_4 = \alpha_{bu}. \end{aligned} \tag{10}$$

Proof. Owing to $\mathbf{I}_L + \rho\mathbf{H}^H(\boldsymbol{\Phi})\mathbf{H}(\boldsymbol{\Phi})$ is a positive definite matrix, the function $\log_2 \det\left(\mathbf{I}_L + \rho\mathbf{H}^H(\boldsymbol{\Phi})\mathbf{H}(\boldsymbol{\Phi})\right)$ is concave. According to the Jensen Inequality, we obtain

$$C(\boldsymbol{\Phi}) \leqslant \log_2 \det\left(\mathbb{E}\left\{\mathbf{I}_L + \rho\mathbf{H}^H(\boldsymbol{\Phi})\mathbf{H}(\boldsymbol{\Phi})\right\}\right). \tag{11}$$

Here, $\mathbb{E}\left\{\mathbf{H}^H(\boldsymbol{\Phi})\mathbf{H}(\boldsymbol{\Phi})\right\}$ can be decomposed by

$$\begin{aligned}&\mathbb{E}\left\{\mathbf{H}^H(\boldsymbol{\Phi})\mathbf{H}(\boldsymbol{\Phi})\right\}\\=&\mathbb{E}\left\{\mathbf{H}_{iu}^H\boldsymbol{\Phi}^H\mathbf{H}_{bi}^H\mathbf{H}_{bi}\boldsymbol{\Phi}\mathbf{H}_{iu}\right\}+\mathbb{E}\left\{\mathbf{H}_{bu}^H\mathbf{H}_{bu}\right\}\\+&\mathbb{E}\left\{\mathbf{H}_{iu}^H\boldsymbol{\Phi}^H\mathbf{H}_{bi}^H\mathbf{H}_{bu}\right\}+\mathbb{E}\left\{\mathbf{H}_{bu}^H\mathbf{H}_{bi}\boldsymbol{\Phi}\mathbf{H}_{iu}\right\}\\=&\mathbb{E}\left\{\mathbf{H}_{iu}^H\boldsymbol{\Phi}^H\mathbf{H}_{bi}^H\mathbf{H}_{bi}\boldsymbol{\Phi}\mathbf{H}_{iu}\right\}+\beta_4M\mathbf{I}_L.\end{aligned}\tag{12}$$

And

$$\begin{aligned}&\mathbb{E}\left\{\mathbf{H}_{iu}^H\boldsymbol{\Phi}^H\mathbf{H}_{bi}^H\mathbf{H}_{bi}\boldsymbol{\Phi}\mathbf{H}_{iu}\right\}\\=&\beta_1\mathbb{E}\{\underbrace{\bar{\mathbf{H}}_{iu}^H\boldsymbol{\Phi}^H\bar{\mathbf{H}}_{bi}^H\bar{\mathbf{H}}_{bi}\boldsymbol{\Phi}\bar{\mathbf{H}}_{iu}}_{\mathbf{Z}_1}\}+\beta_2\mathbb{E}\{\underbrace{\bar{\mathbf{H}}_{iu}^H\boldsymbol{\Phi}^H\tilde{\mathbf{H}}_{bi}^H\tilde{\mathbf{H}}_{bi}\boldsymbol{\Phi}\bar{\mathbf{H}}_{iu}}_{\mathbf{Z}_2}\}\\&+\frac{\alpha_{bi}\alpha_{iu}\mathcal{K}_{bi}}{(\mathcal{K}_{bi}+1)(\mathcal{K}_{iu}+1)}\mathbb{E}\{\underbrace{\tilde{\mathbf{H}}_{iu}^H\boldsymbol{\Phi}^H\bar{\mathbf{H}}_{bi}^H\bar{\mathbf{H}}_{bi}\boldsymbol{\Phi}\tilde{\mathbf{H}}_{iu}}_{\mathbf{Z}_3}\}\\&+\frac{\alpha_{bi}\alpha_{iu}}{(\mathcal{K}_{bi}+1)(\mathcal{K}_{iu}+1)}\mathbb{E}\{\underbrace{\tilde{\mathbf{H}}_{iu}^H\boldsymbol{\Phi}^H\tilde{\mathbf{H}}_{bi}^H\tilde{\mathbf{H}}_{bi}\boldsymbol{\Phi}\tilde{\mathbf{H}}_{iu}}_{\mathbf{Z}_4}\},\end{aligned}\tag{13}$$

where

$$\mathbb{E}\{\mathbf{Z}_1\}=\bar{\mathbf{H}}_{iu}^H\boldsymbol{\Phi}^H\bar{\mathbf{H}}_{bi}^H\bar{\mathbf{H}}_{bi}\boldsymbol{\Phi}\bar{\mathbf{H}}_{iu},\tag{14}$$

$$\mathbb{E}\{\mathbf{Z}_2\}=\bar{\mathbf{H}}_{iu}^H\boldsymbol{\Phi}^H\mathbb{E}\{\tilde{\mathbf{H}}_{bi}^H\tilde{\mathbf{H}}_{bi}\}\boldsymbol{\Phi}\bar{\mathbf{H}}_{iu}=M\bar{\mathbf{H}}_{iu}^H\bar{\mathbf{H}}_{iu},\tag{15}$$

$$\mathbb{E}\{\mathbf{Z}_3\}=MN\mathbf{I}_L,\tag{16}$$

$$\mathbb{E}\{\mathbf{Z}_4\}=\mathbb{E}\{\tilde{\mathbf{H}}_{iu}^H\boldsymbol{\Phi}^H\mathbb{E}\{\tilde{\mathbf{H}}_{bi}^H\tilde{\mathbf{H}}_{bi}\}\boldsymbol{\Phi}\tilde{\mathbf{H}}_{iu}\}=MN\mathbf{I}_L.\tag{17}$$

Here, (16) holds is owing to each non-diagonal element of $\mathbf{Z}_3$ exists Gaussian variables with zero mean. In the end, substituting the results of each part into the original formula, we obtain the final result.

Theorem 1 indicates that the upper bound of ergodic capacity is just related to the matrix $\bar{\mathbf{H}}_{iu}^H\boldsymbol{\Phi}^H\bar{\mathbf{H}}_{bi}^H\bar{\mathbf{H}}_{bi}\boldsymbol{\Phi}\bar{\mathbf{H}}_{iu}$. When applying suitable phase shifts of the IRS, the upper bound of ergodic capacity is also influenced by the distance-dependent path losses and Rician factors.

3.2 Problem Formulation

In this subsection, in order to obtain the optimal phase shifts of the IRS, we formulate an optimization problem (P1) which maximizes the upper bound of ergodic capacity. It is expressed as

$$\begin{aligned}(P1):\ &\max_{\boldsymbol{\Phi}}\ \log_2\det(\rho\beta_1\bar{\mathbf{H}}_{iu}^H\boldsymbol{\Phi}^H\bar{\mathbf{H}}_{bi}^H\bar{\mathbf{H}}_{bi}\boldsymbol{\Phi}\bar{\mathbf{H}}_{iu}\\&\qquad+\rho\beta_2M\bar{\mathbf{H}}_{iu}^H\bar{\mathbf{H}}_{iu}+(1+\rho(\beta_3MN+\beta_4M))\mathbf{I}_L)\\&s.t.\ \theta_{m,n}\in[0,2\pi),m=1,\cdots,N_r,n=1,\cdots,N_c.\end{aligned}\tag{18}$$

The function $\log_2 \det(\mathbf{A})$ is concave when $\mathbf{A}$ is a positive definite matrix, and the matrix in the object function is positive definite. However, the object function is not concave with respect to $\mathbf{\Phi}$. In addition, the constraint of (P1) is equivalent to $|\mathbf{\Phi}_{m,n}| = 1$, which is not convex. Thus, it's not easy to obtain an great solution of this problem.

3.3 Solution

In this subsection, we apply SDR to transport (P1) into a convex problem to solve. At first, we introduce a matrix variable $\mathbf{Y} = \bar{\mathbf{H}}_{iu}^H \mathbf{\Phi}^H \bar{\mathbf{H}}_{bi}^H \bar{\mathbf{H}}_{bi} \mathbf{\Phi} \bar{\mathbf{H}}_{iu}$. Secondly, we denote $\bar{\mathbf{H}}_{iu}$ as a block matrix $\bar{\mathbf{H}}_{iu} = [\bar{\mathbf{H}}_{iu}^1, \ldots, \bar{\mathbf{H}}_{iu}^L]$. Thirdly, we define $\mathbf{R}_j \triangleq \bar{\mathbf{H}}_{bi} \mathrm{diag}(\bar{\mathbf{H}}_{iu}^j) \in \mathbb{C}^{M \times N}$ and $\mathbf{w} \triangleq \mathrm{rvec}(e^{j\mathbf{\Theta}}) \in \mathbb{C}^{1 \times N}$. Thus, we obtain

$$\bar{\mathbf{H}}_{bi} \mathbf{\Phi} \bar{\mathbf{H}}_{iu} = \left[\mathbf{R}_1 \mathbf{w}^H \ \mathbf{R}_2 \mathbf{w}^H \ \cdots \mathbf{R}_L \mathbf{w}^H \right], \tag{19}$$

and

$$\mathbf{Y} = \begin{bmatrix} \mathbf{w}\mathbf{R}_1^H \mathbf{R}_1 \mathbf{w}^H & \mathbf{w}\mathbf{R}_1^H \mathbf{R}_2 \mathbf{w}^H & \cdots & \mathbf{w}\mathbf{R}_1^H \mathbf{R}_L \mathbf{w}^H \\ \mathbf{w}\mathbf{R}_2^H \mathbf{R}_1 \mathbf{w}^H & \mathbf{w}\mathbf{R}_2^H \mathbf{R}_2 \mathbf{w}^H & \cdots & \mathbf{w}\mathbf{R}_2^H \mathbf{R}_L \mathbf{w}^H \\ \vdots & \vdots & \ddots & \vdots \\ \mathbf{w}\mathbf{R}_L^H \mathbf{R}_1 \mathbf{w}^H & \mathbf{w}\mathbf{R}_L^H \mathbf{R}_2 \mathbf{w}^H & \cdots & \mathbf{w}\mathbf{R}_L^H \mathbf{R}_L \mathbf{w}^H \end{bmatrix}. \tag{20}$$

At last, we introduce an hermitian semi-definite matrix $\mathbf{W} = \mathbf{w}^H \mathbf{w} \in \mathbb{C}^{N \times N}$, which satisfies $\mathrm{rank}(\mathbf{W}) = 1$ and $\mathbf{W}_{ii} = 1, i = 1, \cdots, N$. Thus,

$$\begin{aligned} \mathbf{Y}_{ij} &= \mathrm{tr}(\mathbf{w}\mathbf{R}_i^H \mathbf{R}_j \mathbf{w}^H) = \mathrm{tr}(\mathbf{R}_i^H \mathbf{R}_j \mathbf{w}^H \mathbf{w}) \\ &= \mathrm{tr}(\mathbf{R}_i^H \mathbf{R}_j \mathbf{W}), \ i, j = 1, \cdots, L. \end{aligned} \tag{21}$$

In summary, we relax the constraint $\mathrm{rank}(\mathbf{W}) = 1$ and transport (P1) into the following problem (P2)

$$\begin{aligned} (P2): \ \max_{\mathbf{W}, \mathbf{Y}} \ & \log_2 \det(\rho\beta_1 \mathbf{Y} + \rho\beta_2 M \bar{\mathbf{H}}_{iu}^H \bar{\mathbf{H}}_{iu} \\ & + (1 + \rho(\beta_3 MN + \beta_4 M)) \mathbf{I}_L) \\ s.t. \ & \mathbf{Y} = \begin{bmatrix} \mathrm{tr}(\mathbf{R}_1^H \mathbf{R}_1 \mathbf{W}) & \cdots & \mathrm{tr}(\mathbf{R}_1^H \mathbf{R}_L \mathbf{W}) \\ \vdots & \ddots & \vdots \\ \mathrm{tr}(\mathbf{R}_L^H \mathbf{R}_1 \mathbf{W}) & \cdots & \mathrm{tr}(\mathbf{R}_L^H \mathbf{R}_L \mathbf{W}) \end{bmatrix}, \\ & \mathbf{W} \succeq 0, \\ & \mathbf{W}_{ii} = 1, i = 1, \cdots, L. \end{aligned} \tag{22}$$

The problem (P2) is a convex semi-definite program (SDP) problem, we can obtain the optimal solution easily by some convex optimization toolboxes such as CVX [5]. By solving (P2), the optimal solution is about $\mathbf{W}$, then we decompose the optimal $\mathbf{w}$ from the optimal $\mathbf{W}$.

Actually, it is easy to obtain the optimal $\mathbf{w}$ when the optimal $\mathbf{W}$ satisfies $\mathrm{rank}(\mathbf{W}) = 1$. If $\mathrm{rank}(\mathbf{W}) \neq 1$, the optimal solution of problem (P2) is just an

upper bound of the original problem. At this situation, we can obtain the sub-optimal solution by Gaussian random method. At first, the eigenvalue decomposition of $\mathbf{W}$ can be denoted as $\mathbf{W} = \mathbf{U}\mathbf{\Sigma}\mathbf{U}^H$, where $\mathbf{\Sigma} \in \mathbb{C}^{N\times N}$ is a diagonal matrix consists of the eigenvalues of $\mathbf{W}$ and $\mathbf{U} \in \mathbb{C}^{N\times N}$ is composed of the corresponding eigenvectors. Secondly, by generating a random vector $\mathbf{r} \in \mathbb{C}^{1\times N}$ whose elements follow $\mathcal{CN}(0,1)$, we obtain a sub-optimal solution $\mathbf{w} = \mathbf{r}\mathbf{\Sigma}^{\frac{1}{2}}\mathbf{U}^H$. At last, we can choose the best solution by repeating the previous step for a certain number of times. The process of obtaining the optimal $\mathbf{w}$ is show in Algorithm 1.

Algorithm 1. optimal $\mathbf{w}$

initialization set system parameters
obtain the optimal $\mathbf{W}$ by solving Problem (P2)
if rank$(\mathbf{W}) = 1$ **then**
    decomposition: $\mathbf{W} = \mathbf{w}^H\mathbf{w}$
if rank$(\mathbf{W}) \neq 1$ **then**
    eigenvalue decomposition: $\mathbf{W} = \mathbf{U}\mathbf{\Sigma}\mathbf{U}^H$
    repeat
        generate a Gaussian random vector $\mathbf{r}$
        obtain a sub-optimal solution: $\mathbf{w} = \mathbf{r}\mathbf{\Sigma}^{\frac{1}{2}}\mathbf{U}^H$
    until a certain number of times
    choose a $\mathbf{w}$ satisfies that the value of Problem (P1) is the biggest
return $\mathbf{w}$

4 Numerical Result

In this section, the numerical results are given to verify the above theoretical derivation and show the performance of the solution we proposed.

At first, we build an geometric model to describe the positional relationship of the BS, IRS and user in the system, which is shown in Fig. 2. The antennas of the BS and IRS are placed on the high buildings, and the distance between them is denoted by d_{bi}. The user is on the ground, and the distances to the BS are denoted by d_x and d_y, respectively. Thus, the distances from the BS and IRS to the user are denoted by $d_{bu} = \sqrt{d_x^2 + d_y^2}$ and $d_{iu} = \sqrt{(d_{bi} - d_x)^2 + d_y^2}$, respectively.

In addition, the distance-dependent path loss is given by

$$\alpha = \alpha_0 \left(\frac{d}{d_0}\right)^{-\eta}, \tag{23}$$

where η denotes the fading factor and α_0 denotes the relative power at the distance of d_0. Thus, the corresponding power at the distance of d is α. In the simulation, the main parameters are set in Table 1.

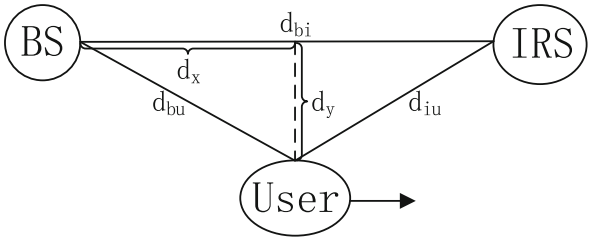

Fig. 2. Simulation model

Table 1. Simulation parameters.

BS antennas ($M_r \times M_c$)	4×8	IRS elements ($N_r \times N_c$)	8×8
Rician factor ($\mathcal{K}_{bi}$)	1	Rician factor ($\mathcal{K}_{iu}$)	1
Vertical AoD ($\delta_{bi}^{(v)}$)	90°	Vertical AoA ($\gamma_{bi}^{(v)}$)	90°
Vertical AoD ($\delta_{iu}^{(v)}$)	45°	Vertical AoA ($\gamma_{iu}^{(v)}$)	45°
Horizontal AoD ($\delta_{bi}^{(h)}$)	90°	Horizontal AoA ($\gamma_{bi}^{(h)}$)	90°
Horizontal AoD ($\delta_{iu}^{(h)}$)	$\arccos \frac{d_y}{d_{iu}}$	Horizontal AoA ($\gamma_{iu}^{(h)}$)	$\arcsin \frac{d_y}{d_{iu}}$
Distance (d_{bi})	100 m	Distance (d_y)	20 m
Path loss (α_0)	−10 dB	Distance (d_0)	100 m
Fading factor (η)	2	SNR	20 dB

4.1 Ergodic Capacity

In this subsection, We apply the optimal solution to compare the upper bound of ergodic capacity of the system with 1000000 times Monte Carlo results. The result is shown in Fig. 3, d_x changes with the user's movement in the horizontal direction. Thus, the distance-dependent path loss changes accordingly.

We set $L = 1(1 \times 1)$, $L = 2(1 \times 2)$ and $L = 3(1 \times 3)$ respectively to show the gap. When $L = 1$, the two curves are very close. And the gap enlarges as the number of user's antennas L increases. It is worth noticing that the gap stays unchanged as d_x varies. Thus, we can obtain better solution by optimizing the upper bound of the ergodic capacity of the system.

4.2 Optimal Solution

In this subsection, we set a few groups of phase shifts to compare with each other and verify the advantage of our proposed solution. The results are shown in Figs. 4 and 5, we consider two situations where $L = 2(1 \times 2)$ and $L = 3(1 \times 3)$. The performances of applying random phase shifts and optimal phase shifts are shown. Here the results of applying random phase shifts are obtained by choosing the best performance of 10000 types results with different random phase shifts. In addition, the performance without IRS is also shown as a baseline.

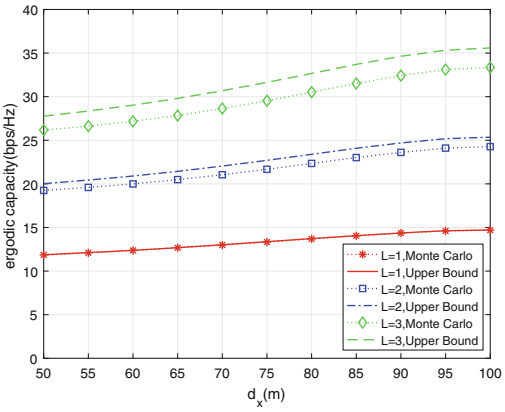

Fig. 3. Upper bound of ergodic capacity and Monte Carlo results

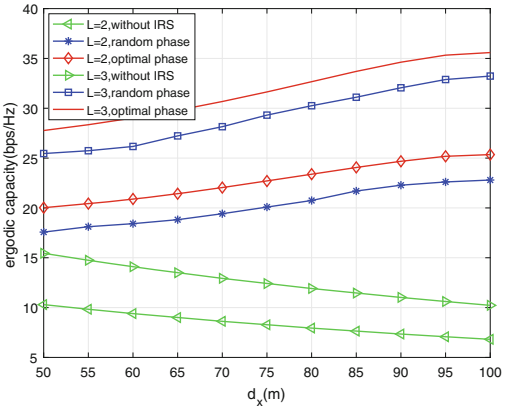

Fig. 4. Performance of optimal solution with d_x

From Figs. 4 and 5, we see that the performance of the IRS-assisted system is significantly better than the system without IRS. The 10000 results with random phase shifts can not achieve the performance of applying optimal phase shifts. The ergodic capacity decreases with the increase of d_x, due to that the power attenuation intensifies as the distance between the BS and the user grows. On the contrary, the ergodic capacity of the IRS-assisted system increases, due to that IRS provides more signal energy gains. Besides, the gap between random phase shifts and optimal phase shifts enlarges as N increases, indicating that applying optimal phase shifts is significant when N is relatively large.

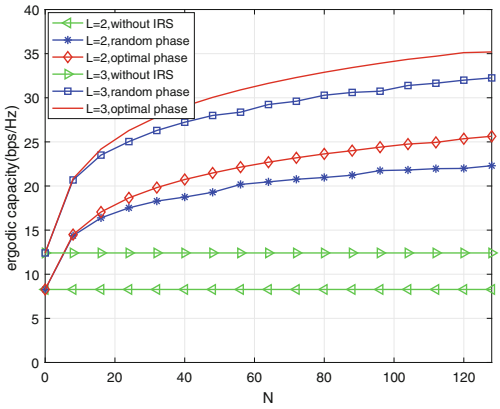

Fig. 5. Performance of optimal solution with N

4.3 Performance of Multiple Receive Antennas

In this subsection, we show the performance gains provided by multiple antennas. We apply the optimal phase shifts of IRS and compare the performance with different receive antennas.

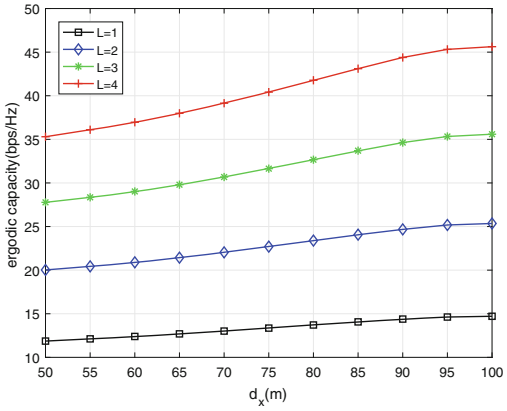

Fig. 6. Performance of multiple receive antennas with d_x

The result is shown in Figs. 6 and 7, we set $L = 1(1 \times 1)$, $L = 2(1 \times 2)$, $L = 3(1 \times 3)$ and $L = 4(2 \times 2)$, respectively. It is obviously that the ergodic capacity grows a lot as the receive antennas L increases. Therefore, applying multi-antenna at the user helps improve the signal quality of the IRS-assisted system. In addition, with the increase of N, the performance advantages of system are more significant.

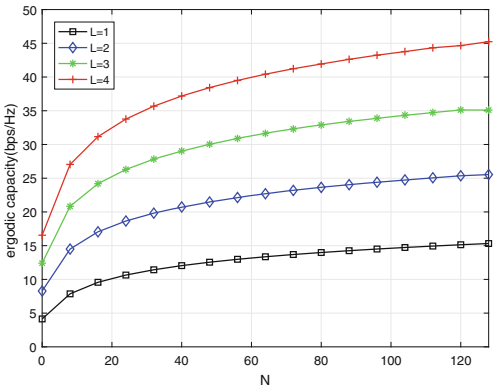

Fig. 7. Performance of multiple receive antennas with N

5 Conclusion

In this paper, we analyze the ergodic capacity of the IRS-assisted MIMO wireless communication system. We give the upper bound of ergodic capacity and maximize it to obtain the optimal phase shifts of IRS. We apply SDR method to transform the original problem into a convex SDP problem and solve it by CVX. By applying Gaussian random method, we decompose the optimal or suboptimal phase shifts from the optimal solution. At last, we show the advantages of our proposed solution and the performance gains provided by multiple antennas through the numerical simulation.

References

1. Boccardi, F., Heath, R.W., Lozano, A., Marzetta, T.L., Popovski, P.: Five disruptive technology directions for 5G. IEEE Commun. Mag. **52**(2), 74–80 (2014)
2. Carrasco, E., Perruisseau-Carrier, J.: Reflectarray antenna at terahertz using graphene. IEEE Antennas Wirel. Propag. Lett. **12**(3), 253–256 (2013)
3. Chen, J., Liang, Y.C., Pei, Y., Guo, H.: Intelligent reflecting surface: a programmable wireless environment for physical layer security. arXiv preprint arXiv:1905.03689 (2019)
4. Foschini, G.J., Gans, M.J.: On limits of wireless communications in a fading environment when using multiple antennas. Wirel. Pers. Commun. **6**(3), 311–335 (1998)
5. Grant, M., Boyd, S., Ye, Y.: CVX: Matlab software for disciplined convex programming (2008)
6. Han, Y., Tang, W., Jin, S., Wen, C.K., Ma, X.: Large intelligent surface-assisted wireless communication exploiting statistical CSI (2018)
7. Hu, S., Rusek, F., Edfors, O.: Beyond massive MIMO: the potential of data transmission with large intelligent surfaces. IEEE Trans. Sig. Process. **66**(10), 2746–2758 (2018)
8. Hu, W., et al.: Design and measurement of reconfigurable millimeter wave reflectarray cells with nematic liquid crystal. IEEE Trans. Antennas Propag. **56**(10), 3112–3117 (2008)

9. Huang, C., Zappone, A., Alexandropoulos, G.C., Debbah, M., Yuen, C.: Large intelligent surfaces for energy efficiency in wireless communication (2018)
10. Huang, C., Zappone, A., Debbah, M., Yuen, C.: Achievable rate maximization by passive intelligent mirrors (2018)
11. Hum, S.V., Perruisseaucarrier, J.: Reconfigurable reflectarrays and array lenses for dynamic antenna beam control: a review. IEEE Trans. Antennas Propag. **62**(1), 183–198 (2014)
12. Larsson, E.G., Edfors, O., Tufvesson, F., Marzetta, T.L.: Massive mimo for next generation wireless systems. IEEE Commun. Mag. **52**(2), 186–195 (2014)
13. Lu, L., Li, G.Y., Swindlehurst, A.L., Ashikhmin, A., Zhang, R.: An overview of massive MIMO: benefits and challenges. IEEE J. Sel.d Top. Sig. Process. **8**(5), 742–758 (2014)
14. Subrt, L., Pechac, P.: Intelligent walls as autonomous parts of smart indoor environments. IET Commun. **6**(8), 1004–1010 (2012)
15. Wu, Q., Li, G.Y., Chen, W., Ng, D.W.K., Schober, R.: An overview of sustainable green 5G networks. IEEE Wirel. Commun. **24**(4), 72–80 (2017)
16. Wu, Q., Zhang, R.: Intelligent reflecting surface enhanced wireless network: joint active and passive beamforming design (2018)
17. Xin, T., Zhi, S., Jornet, J.M., Pados, D.: Increasing indoor spectrum sharing capacity using smart reflect-array. Mathematics (2015)
18. Yu, X., Xu, D., Schober, R.: Enabling secure wireless communications via intelligent reflecting surfaces. arXiv preprint arXiv:1904.09573 (2019)